Applied Physics Letters ARTICLE pubs.aip.org/aip/apl

Anomalous interlayer vibrations in few-layer InSe induced by weak intralayer bonding

Cite as: Appl. Phys. Lett. **123**, 053103 (2023); doi: 10.1063/5.0166258
Submitted: 4 July 2023 · Accepted: 17 July 2023 ·
Published Online: 3 August 2023

View Online Export Citation CrossMark

Heng Wu,[1,2] Yan Zhou,[1] Yu-Xin Cai,[3] Miao-Ling Lin,[1] Lijun Zhang,[3] and Ping-Heng Tan[1,2,a)]

AFFILIATIONS

[1]State Key Laboratory of Superlattices and Microstructures, Institute of Semiconductors, Chinese Academy of Sciences, Beijing 100083, China
[2]Center of Materials Science and Optoelectronics Engineering & CAS Center of Excellence in Topological Quantum Computation, University of Chinese Academy of Sciences, Beijing 100049, China
[3]State Key Laboratory of Integrated Optoelectronics, Key Laboratory of Automobile Materials of MOE, International Center of Computational Method and Software, School of Materials Science and Engineering, Jilin University, Changchun 130012, China

[a)]Author to whom correspondence should be addressed: phtan@semi.ac.cn

ABSTRACT

Atomically thin InSe is a promising semiconductor that possesses exceptional plasticity, high electron mobility, and wide bandgap tunability, which are thought to be highly sensitive to interlayer coupling. Since the interlayer vibration modes can provide direct access to the interlayer coupling strength, in this study, we systematically investigated the interlayer modes in few-layer InSe using low-frequency Raman spectroscopy. We found that the commonly used linear chain model (LCM), which treats the single layer as a rigid entity, is inadequate in accurately describing the frequencies of interlayer shear modes in InSe due to the influence of weak in-plane intralayer In–In bonding. This issue can be addressed with a modified model that accounts for both the in-plane interlayer coupling between InSe layers and the in-plane intralayer interaction within InSe layers. However, the out-of-plane intralayer In–In bonding is strong enough so that it has negligible impact on the frequency of the interlayer layer-breathing modes, which can be well understood by the LCM. Our study reveals how the weak intralayer bonding in two-dimensional materials gives a non-negligible contribution to the corresponding interlayer vibrations.

Over the past decade, the discovery of graphene has spurred the exploration of other two-dimensional materials (2DMs) for promising electronic and optoelectronic applications.[1] Among them, InSe, a representative of the III–VI layered compounds, has attracted increasing interest due to its exceptional deformability and plasticity, high electron mobility, and tunable bandgap across a wide spectral range.[2,3] These properties, which are strongly correlated with interlayer coupling, make InSe a promising material for flexible electronics and optoelectronic devices.[4] Therefore, a detailed investigation of the interlayer coupling properties of InSe is crucial for a comprehensive understanding of the material's intrinsic physical properties and the design of InSe-based vdWHs.

The interlayer coupling properties of 2DMs can be determined by analyzing the electronic and vibrational properties with respect to their layer number.[4] Raman spectroscopy as one of the available techniques provides nondestructive and quick optical insight into the vibration modes of 2DMs.[5–7] Particularly, the interlayer modes, including the in-plane shear (S) modes and out-of-plane layer-breathing (LB) modes, are highly sensitive to the layer number and interfacial stacking conditions (e.g., twist stacking and hetero-stacking), and therefore, can serve as valuable probes for studying interlayer/interfacial coupling.[8–10] Due to the fact that the intralayer bonding is typically much stronger than the interlayer van der Waals force, the frequency of layer-number dependent interlayer modes in various 2DMs can be well understood with the linear chain model (LCM), which treats the single layer as a rigid entity. In this case, the materials can be regarded as spring-connected rigid entities in which only nearest-neighbor interactions are taken into account.[11,12] The LCM can well explain the frequency of layer-dependent interlayer modes of most 2DMs. A few exceptions include the twisted multilayer graphene and certain 2DMs with multiple atomic layers, such as Bi_2Se_3 and Bi_2Te_3.[13,14] The former requires consideration of next-nearest-neighbor interactions, while the latter is proved to have strong coupling to the substrate and, therefore, both require corrections to the LCM. In addition, when the frequencies of intralayer modes are close to those of interlayer modes, i.e., the intralayer bonding as

weak as van der Waals force, the single layer cannot be treated as a rigid entity. The interlayer vibrations of 2DMs with weak intralayer bonding still remain unclear.

In this work, we systematically investigated the interlayer vibrations in few-layer ε-phase InSe using low-frequency Raman spectroscopy. In contrast to the common 2DMs, a weak in-plane intralayer In-In bonding exists in InSe resulting in an $E''(1)$ mode at ~40 cm^{-1} and we found that the widely used LCM overestimates the S mode frequencies of InSe. This deviation was corrected by a modified LCM (MLCM) after considering both inter- and intralayer interactions. The LB modes are absent in the Raman spectra of InSe while several LB modes were observed in InSe/$MoTe_2$ vdWHs, exhibiting different peak positions from that of the $MoTe_2$ constituent. On the contrary, we found the common LCM can well explain the LB mode frequencies of InSe/$MoTe_2$ vdWHs and the deduced LB mode frequency of bulk InSe agrees well with that calculated by density functional theory (DFT). This was attributed to the stronger out-of-plane intralayer In–In bonding as revealed by the higher frequency of the $A_1'(1)$ mode than that of the $E''(1)$ mode. Our finding not only provides an approach for accurately determining the thickness of InSe but also helps to understand the interlayer coupling properties of other 2DMs with weak intralayer bonding.

We first characterized the general vibration properties of both few-layer and bulk InSe. The ε-InSe crystal has a hexagonal layered structure and each layer consists of four atomic layers arranged in the sequence of Se–In–In–Se, as illustrated in Fig. 1(a). Few-layer ε-InSe flakes were exfoliated onto SiO_2/Si substrate, whose thickness was determined by atomic force microscopy and crystal phase was verified by high-resolution transmission electron microscopy (see Fig. S1 in the supplementary material). Since monolayer and bulk ε-InSe retain a point group of D_{3h}, the corresponding representation of phonons at Γ point are $\Gamma_{Mono} = 2A_1' + 2A_2'' + 2E' + 2E''$ and $\Gamma_{Bulk} = 4A_1' + 4A_2'' + 4E' + 4E''$, respectively.[4,15,16] The atomic displacement of each intralayer mode in monolayer InSe is illustrated in Fig. 1(b). Figure 1(c) shows the Raman spectra of 5-layer (5L), 8-layer (8L), and bulk InSe with an excitation energy (E_{ex}) of 2.33 eV. All the intralayer modes are observed, including $E''(1)$ at ~40 cm^{-1}, $A_1'(1)$ at ~115 cm^{-1}, $E'(1)$ TO/$E''(2)$ at ~178 cm^{-1}, $A_2''(1)$ TO at ~196 cm^{-1}, $A_2''(1)$ LO at ~199 cm^{-1}, and $A_1'(2)$ at ~227 cm^{-1}.

The $A_2''(1)$ LO/TO modes can only be observed in few-layer InSe, indicating its reduced symmetry. Apart from the intralayer modes, the low-frequency interlayer modes below 20 cm^{-1} can also be observed, which is consistent with the previous reports.[17,18] It is noteworthy that the frequency of the $E''(1)$ mode is merely 40 cm^{-1}, which is comparable to that of interlayer modes in certain 2DMs, such as the LB mode in 2L-MoS_2.[12] The $E''(1)$ mode originates from the in-plane relative motion between the top and bottom Se–In diatomic layers within the monolayer InSe. Its low frequency suggests weak in-plane In–In bonding in InSe. This is also supported by the degenerate frequencies of the $E''(2)$ and $E'(1)$ TO modes at 178 cm^{-1}, since the difference between their atomic displacements is the direction of relative motion of the top and bottom Se–In diatomic layers. Additionally, the $E''(1)$ mode of multilayer InSe exhibits a frequency splitting, i.e., Davydov splitting, as shown in the inset to Fig. 1(c).

To investigate the influence of weak in-plane intralayer In–In bonding on the interlayer mode frequency of InSe, we redirected our focus toward the interlayer modes below 20 cm^{-1}. Raman spectra of 5L-InSe with four excitation energies (E_{ex}) are depicted in Fig. 1(d). When E_{ex} (2.54 eV) is close to the B exciton energy of 5L-InSe (~2.50 eV),[2] the photo-excited carriers result in a background near the Rayleigh line and obscures the low-frequency Raman signal of interest. Thus, $E_{ex} = 2.33$ eV was selected to avoid such background and get better signal-to-noise of the interlayer modes because the B exciton energy of 1–10L InSe decreases from ~2.90 to ~2.45 eV.[2,19] Polarized Raman spectroscopy in Fig. 1(e) was used to assign the observed interlayer modes. Based on the symmetry analysis, the S modes of InSe can be detected in both parallel-polarization (VV) and cross-polarization (HV) configurations, while the LB modes can only be detected in the VV configuration[6] (see Sec. IV in the supplementary material for detail). All the observed modes below 20 cm^{-1} were identified as S modes, and they exhibit substantial intensity variations at different positions (see Fig. S2 in the supplementary material) as also reported in γ-InSe,[18] which indicates different stacking sequences of InSe flakes at different positions, similar to the case of GaSe flakes.[20] However, the unchanged frequency of each S mode at different positions (see Fig. S2 in the supplementary material) indicates the same strength of in-plane interlayer coupling within InSe flakes with different stacking sequences.

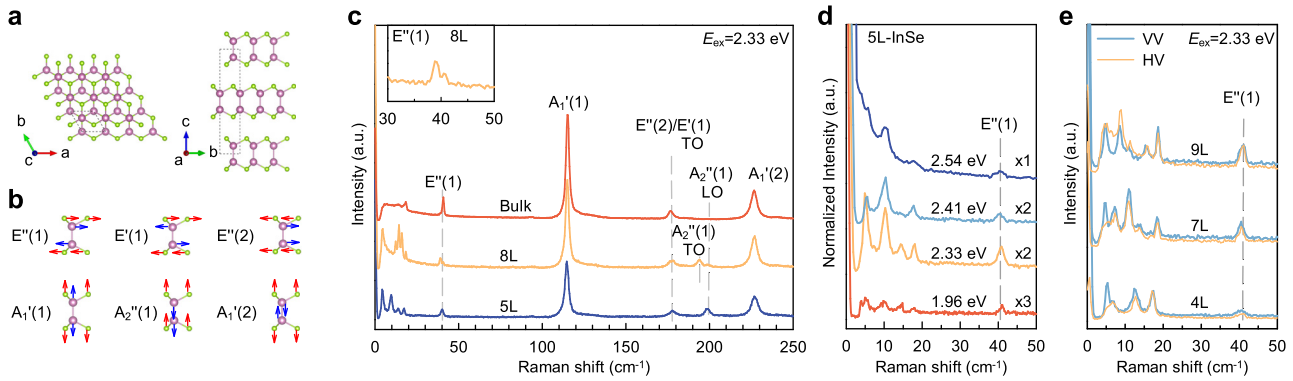

FIG. 1. (a) Schematic structure of ε-InSe, with both the top and side views. (b) Atomic displacements of the intralayer modes of InSe. (c) Raman spectra of few-layer and bulk InSe. The blue box highlights the interlayer modes of InSe. Inset: the mode splitting of the $E''(1)$ mode of 8L-InSe. (d) Raman spectra of 5L-InSe with four different E_{ex}. (e) Polarized Raman spectra of 4L-, 7L-, and 9L-InSe under VV (thick lines)/HV (thin lines) configurations.

We continue to analyze the layer-number dependent S mode frequencies of InSe to estimate the strength of in-plane interlayer coupling. The frequencies of interlayer modes can be explained by the LCM,[11,12] and the eigenfrequencies of the S modes in NL-InSe can be expressed as[11,12]

$$\omega(\mathrm{S}_{N,N-j}) = \omega(\mathrm{S}_{\mathrm{bulk}}) \sin\left(\frac{j\pi}{2N}\right), \tag{1}$$

where $\omega(\mathrm{S}_{\mathrm{bulk}})$ is the S mode frequency of bulk InSe and $j = 1, 2, \ldots, N-1$, and $\mathrm{S}_{N,1}$ denotes the S mode with the highest frequency. The in-plane interlayer constant ($\alpha^{\parallel}$) in InSe is given by $\omega(\mathrm{S}_{\mathrm{bulk}}) = \sqrt{\alpha^{\parallel}/\pi^2 c^2 \mu}$, where $c = 3 \times 10^8 \mathrm{m \cdot s^{-2}}$ is the speed of light, $\mu = 4.53 \times 10^{-6} \mathrm{kg \cdot m^{-2}}$ is the mass per unit area of monolayer InSe, and $\omega(S_{\mathrm{bulk}})$ is 18.9 $\mathrm{cm^{-1}}$ in Fig. 1(d). The $\alpha^{\parallel}$ is calculated to be $1.44 \times 10^{19} \mathrm{N \cdot m^{-3}}$.

The frequencies of both S modes and $E''(1)$ modes of 2–10L InSe in Fig. 2(a) are summarized in Fig. 2(b) along with the corresponding calculated S mode frequencies based on Eq. (1). The schematic diagram of the LCM for multilayer InSe is illustrated in the inset to Fig. 2(b). Unexpectedly, Fig. 2(b) shows that the LCM-based results overestimate the S mode frequencies for 2–10L InSe. Previous reports suggested that the next-nearest-neighbor interaction and substrate–material interaction may lead to frequency discrepancies from LCM.[13,14,21] However, the next-nearest-neighbor interaction will not change the $\mathrm{S}_{N,1}$ frequency but will increase the calculated $\mathrm{S}_{N,2}$ frequency,[13] which is not consistent with the present experimental results. In addition, the substrate–material interaction can be easily excluded since the S mode frequency of supported and suspended InSe are almost the same (see Fig. S3 in the supplementary material). The LCM assumes that each layer of 2DMs is a rigid entity because the strength of interlayer chemical bonding is much larger than the van der Waals force. This assumption may be invalid due to the weak in-plane In–In bonding in InSe and, thus, will lead to discrepancy between the experimental S mode frequencies and the corresponding ones based on the LCM. Therefore, we improved the LCM to treat the monolayer InSe as two rigid In–Se diatomic sublayers, which is denoted as the modified LCM (MLCM). In this model, both the in-plane interlayer interaction and intralayer interaction between adjacent sublayers are considered. The mass per unit area of In–Se sublayer is $\mu_0 = \mu/2 = 2.27 \times 10^{-6} \mathrm{kg \cdot m^{-2}}$. The in-plane interlayer force constant between InSe layers is $\alpha^{\parallel}_{\mathrm{inter}}$ and the in-plane intralayer force constant between In-Se sublayers is $\alpha^{\parallel}_{\mathrm{intra}}$. The S mode frequency of NL-InSe can be calculated by solving a linear homogeneous equation:[10]

$$\omega_j^2 \mathbf{M}\mathbf{u}_j = \frac{1}{4\pi^2 c^2} \mathbf{D}\mathbf{u}_j, \tag{2}$$

where $j = 1, 2, \ldots, (2N-1)$, and $\mathbf{u}_j$ is the phonon eigenvector of the jth mode with frequency ω_j. $\mathbf{M}$ is the $(2N \times 2N)$ diagonal mass matrix and $\mathbf{D}$ is the $(2N \times 2N)$ tridiagonal force constant matrix. ω_j is arranged in sequence according to the frequency, where ω_1 has the lowest frequency. Therefore, the frequency of the $(N-1)$ S modes in NL InSe are ω_1, ω_2,…, ω_{N-1}, and the other ω_j are the frequencies of N Davydov components of intralayer $E''(1)$ in NL InSe.

The MLCM for few-layer InSe is illustrated in the inset to Fig. 2(c). The corresponding calculated frequencies of the S modes and Davydov components of $E''(1)$ mode are depicted in Fig. 2(c) along with the experimental data. The calculated S mode frequencies for 4–10L InSe agree with the experimental data, and the parameters $\alpha^{\parallel}_{\mathrm{inter}}$ and $\alpha^{\parallel}_{\mathrm{intra}}$ are fitted to be 1.48×10^{19} and $6.00 \times 10^{19} \mathrm{N \cdot m^{-3}}$, respectively. The calculated frequencies of the Davydov components of $E''(1)$ also match the experimental ones. Indeed, the in-plane intralayer In–In bonding is about four times larger than the in-plane interlayer coupling, in contrast to the case of the common 2DMs like MoS_2 and $MoTe_2$, whose intralayer force constants are 1–2 orders of magnitude larger than the interlayer force constants.[12,22] Therefore, such weak in-plane interlayer In–In bonding has a non-negligible impact on the S mode frequencies. For 2L- and 3L-InSe, the experimental frequencies of the S modes are significantly lower than the calculated ones, manifesting smaller $\alpha^{\parallel}_{\mathrm{inter}}$ in 2L- and 3L-InSe. Since the strength of interlayer interaction is directly related to the interlayer distance and the interlayer charge distribution, we calculated the interlayer distance and differential charge density for 2–5L and bulk InSe by DFT (see Sec. I in the supplementary material for detail), as shown in Figs. 3(a) and 3(b), respectively. The interlayer distance slightly decreases with the increasing layer number. However, 2 and 3L show less charge accumulation and depletion than other layers, which indicates weaker interlayer interaction.

The atomic displacements of $A_1'(1)$ mode are similar to that of $E''(1)$ mode but along the out-of-plane direction, which may influence the frequencies of LB modes. However, since all the out-of-plane intralayer modes have higher frequencies than that of $E''(1)$ mode, the out-of-plane In–In bonding strength ($\alpha^{\perp}_{\mathrm{intra}}$) should be much larger than that ($\alpha^{\perp}_{\mathrm{inter}}$) of LB interlayer coupling, unlike the case of $\alpha^{\parallel}_{\mathrm{intra}}$ for in-plane In–In bonding. To reveal whether the out-of-plane In–In bonding has an impact on the LB mode frequencies of InSe, we estimated $\alpha^{\perp}_{\mathrm{intra}}$ and $\alpha^{\perp}_{\mathrm{inter}}$ from the corresponding MLCM. Since no LB modes

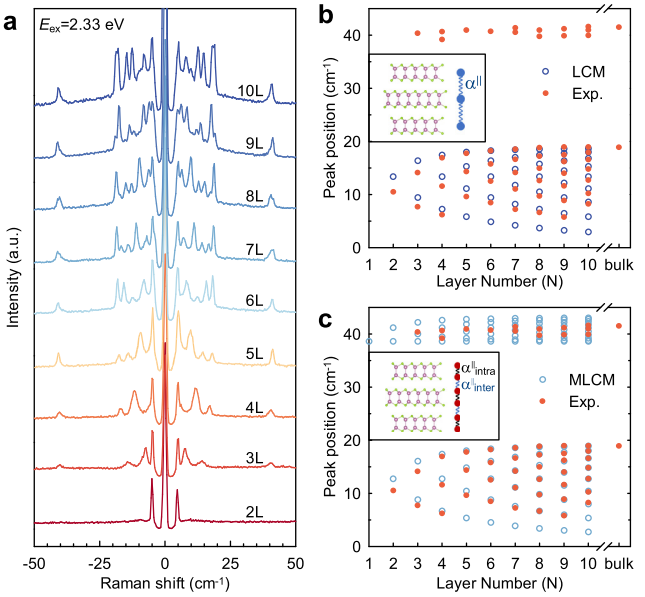

FIG. 2. (a) Low-frequency Raman spectra of 2–10L InSe. (b) Experimental frequencies of S modes, $E''(1)$ modes (dots), and calculated frequencies of S modes by LCM (circles). Inset: schematic diagram of LCM for InSe. (c) Experimental frequencies of S modes, $E''(1)$ modes (dots), and the corresponding calculated frequencies by MLCM (circles). Inset: schematic diagram of MLCM for InSe.

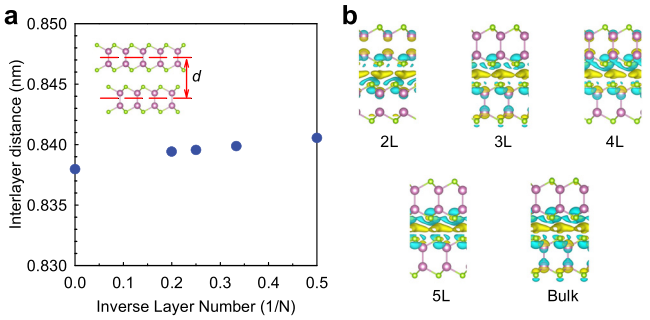

FIG. 3. (a) Interlayer distance of 2–5L and bulk InSe. (b) Interlayer differential charge density of 2–5L and bulk InSe. The isosurface value is set to be 1×10^{-4} electrons $\cdot$Å^{-3}. The charge accumulation and depletion layers are marked in yellow and cyan.

can be clearly observed in Fig. 2(a), we fabricated InSe/$MoTe_2$ vdWHs to access the information of LB modes of InSe, as the case for graphene and hBN.[10] The interfacial coupling allows the LB modes of InSe/$MoTe_2$ vdWHs to couple with the electronic states in $MoTe_2$ constituent and, thus, enables these LB modes to be observed.[9] Figure 4(a) depicts the Raman spectra of 3L-$MoTe_2$, 8L-InSe, and 8L-InSe/3L-$MoTe_2$ with $E_{ex} = 2.33$ eV. The inset shows the optical image of the

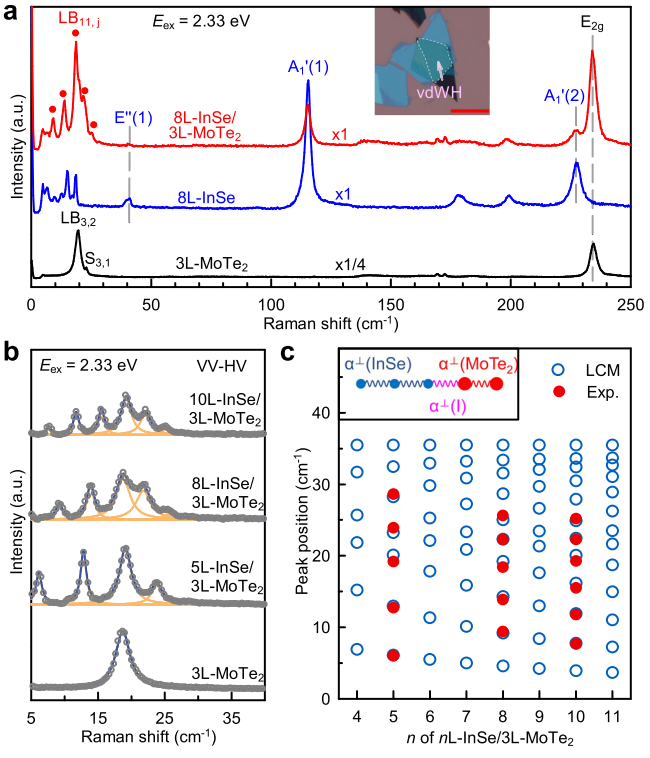

FIG. 4. (a) Raman spectra of 3L-$MoTe_2$, 8L-InSe, and 8L-InSe/3L-$MoTe_2$ with $E_{ex} = 2.33$ eV. The dots indicate the LB modes of vdWHs. Inset: The optical image of 8L-InSe/3L-$MoTe_2$ (vdWH). Scale bar: 20 μm. (b) Raman spectra (circles) and Lorentz fitting (solid lines) of the LB modes in nL-InSe/3L-$MoTe_2$ with different n. (c) The frequencies of LB modes from Raman measurements (exp., dots) and calculation based on LCM (circles).

corresponding vdWH. The high-frequency modes of the vdWH beyond 100 cm^{-1} come from the intralayer modes of InSe and $MoTe_2$ constituents. The emergent low-frequency modes labeled as dots in Fig. 4(c) are assigned as the LB modes in vdWHs. The lattice mismatch between InSe (4.05 Å) and $MoTe_2$ (3.57 Å) is 11.9%, which makes it difficult to form Moiré structures. As a result, we did not discuss the angle dependence of the S and LB modes of vdWHs. One can distinguish the S and LB modes of the vdWHs by polarized Raman measurements since they have different symmetries and the LB mode can be revealed in VV–HV Raman spectra.[23] Therefore, the VV–HV Raman spectra of 3L-$MoTe_2$ and nL-InSe/3L-$MoTe_2$ in Fig. 4(b) depicts the evolution of the LB modes of nL-InSe/3L-$MoTe_2$ vdWHs.

According to the LB mode frequencies of nL-InSe/3L-$MoTe_2$ vdWHs, we used the LCM to extract the LB force constants of InSe [$\alpha^{\perp}$(InSe)] and the interfacial LB force constants of vdWHs [$\alpha^{\perp}$(InSe/$MoTe_2$)]. The inset to Fig. 4(c) depicts the schematic diagram of the LCM for InSe/$MoTe_2$ vdWHs. Based on the corresponding LB force constants of $\alpha^{\perp}(MoTe_2) = 7.8 \times 10^{19}$N $\cdot$ m^{-3} and mass per area of $\mu(MoTe_2) = 5.32 \times 10^{-6}$kg $\cdot$ m^{-3},[10,22] the calculated results are $\alpha^{\perp}$(InSe) $= 4.40 \times 10^{19}$N $\cdot$ m^{-3} and $\alpha^{\perp}$(InSe/$MoTe_2$) $= 2.68 \times 10^{19}$ N $\cdot$ m^{-3}. Figure 4(c) shows the experimental and calculated frequencies of LB modes for the mL-InSe/3L-$MoTe_2$ vdWHs (results for other InSe/$MoTe_2$ vdWHs can be found in Sec. V of the supplementary material). The experimental frequencies match well with the calculated ones. According to the extracted $\alpha^{\perp}$(InSe), the LB mode frequency of bulk InSe is $\omega(LB_{bulk}) = \sqrt{\alpha^{\perp}(InSe)/\pi^2 c^2 \mu} = 33.0$ cm^{-1}, which agrees well with the theoretical one (32.8 cm^{-1}) calculated by DFT. This manifests that the out-of-plane In–In bonding has little impact on the LB modes of InSe. To further prove this point, we also utilize the MLCM to fit the force constant of out-of-plane In–In bonding ($\alpha^{\perp}_{intra}$) with $\omega(A_1'(1)_{bulk}) = 115$ and $\omega(LB_{bulk}) = 32.8$ cm^{-1}. $\alpha^{\perp}_{inter} = 4.35 \times 10^{19}$ and $\alpha^{\perp}_{intra} = 5.10 \times 10^{20}$N $\cdot$ m^{-3} are obtained. The former is one magnitude smaller than the latter, similar to the case of common 2DMs. Thus, it is precise enough for the LCM to deal with evolution of the LB mode frequency of multilayer InSe with layer number.

In conclusion, we investigated the influence of weak intralayer bonding on the interlayer modes of ε-InSe. The weak in-plane In–In bonding makes the in-plane intralayer force constants between adjacent In atomic layers of InSe comparable with the in-plane interlayer force constant. We reveal that this weak intralayer bonding should be considered to accurately explain the frequencies of the S modes. In contrast, the case is quite different for LB modes since the force constant of out-of-plane intralayer In–In bonding is one order of magnitude larger than the out-of-plane interlayer force constant. Our findings shed light on the interlayer coupling properties of InSe and reveal that weak intralayer interaction may lead to frequency discrepancies in the LCM for describing interlayer modes of 2DMs, such as Bi_2Se_3, Bi_2Te_3, and $MnBi_2Te_4$, in which the intralayer modes below 50 cm^{-1} were observed.[14,21,24]

See the supplementary material for the experimental methods, characterization of few-layer InSe sample, extended data for S mode properties in few-layer InSe, symmetry analysis of interlayer Raman modes in few-layer InSe and InSe/$MoTe_2$ vdWHs, and extended data for analysis of LB modes in vdWHs.

This work was supported by the National Natural Science Foundation of China (Grant Nos. 12004377, 11874350, and

12204472), the CAS Key Research Program of Frontier Sciences (Grant Nos. ZDBSLY-SLH004 and XDPB22), and the CAS Project for Young Scientists in Basic Research (Grant No. YSBR-026). Calculations were performed in part at the high-performance computing center of Jilin University.

AUTHOR DECLARATIONS

Conflict of Interest

The authors have no conflicts to disclose.

Author Contributions

Heng Wu: Data curation (equal); Formal analysis (lead); Methodology (equal); Validation (equal); Writing – original draft (equal); Writing – review & editing (equal). **Yan Zhou:** Formal analysis (supporting); Resources (equal); Writing – review & editing (equal). **Yu-Xin Cai:** Software (equal); Writing – review & editing (equal). **Miao-Ling Lin:** Formal analysis (equal); Funding acquisition (equal). **Lijun Zhang:** Software (equal); Supervision (equal); Writing – review & editing (equal). **Ping-Heng Tan:** Conceptualization (lead); Formal analysis (equal); Funding acquisition (equal); Methodology (equal); Project administration (lead); Resources (equal); Supervision (lead); Writing – original draft (equal); Writing – review & editing (equal).

DATA AVAILABILITY

The data that support the findings of this study are available from the corresponding author upon reasonable request.

REFERENCES

[1]K. S. Novoselov, A. K. Geim, S. V. Morozov, D. Jiang, Y. Zhang, S. V. Dubonos, I. V. Grigorieva, and A. A. Firsov, "Electric field effect in atomically thin carbon films," Science **306**, 666–669 (2004).

[2]D. A. Bandurin, A. V. Tyurnina, G. L. Yu, A. Mishchenko, V. Zólyomi, S. V. Morozov, R. K. Kumar, R. V. Gorbachev, Z. R. Kudrynskyi, S. Pezzini, Z. D. Kovalyuk, U. Zeitler, K. S. Novoselov, A. Patanè, L. Eaves, I. V. Grigorieva, V. I. Fal'ko, A. K. Geim, and Y. Cao, "High electron mobility, quantum Hall effect and anomalous optical response in atomically thin InSe," Nat. Nanotechnol. **12**, 223–227 (2017).

[3]T.-R. Wei, M. Jin, Y. Wang, H. Chen, Z. Gao, K. Zhao, P. Qiu, Z. Shan, J. Jiang, R. Li, L. Chen, J. He, and X. Shi, "Exceptional plasticity in the bulk single-crystalline van der Waals semiconductor InSe," Science **369**, 542–545 (2020).

[4]Y. Sun, S. Luo, X.-G. Zhao, K. Biswas, S.-L. Li, and L. Zhang, "InSe: A two-dimensional material with strong interlayer coupling," Nanoscale **10**, 7991–7998 (2018).

[5]X. Zhang, X.-F. Qiao, W. Shi, J.-B. Wu, D.-S. Jiang, and P.-H. Tan, "Phonon and Raman scattering of two-dimensional transition metal dichalcogenides from monolayer, multilayer to bulk material," Chem. Soc. Rev. **44**, 2757–2785 (2015).

[6]L. Liang, J. Zhang, B. G. Sumpter, Q.-H. Tan, P.-H. Tan, and V. Meunier, "Low-frequency shear and layer-breathing modes in Raman scattering of two-dimensional materials," ACS Nano **11**, 11777–11802 (2017).

[7]J.-B. Wu, M.-L. Lin, X. Cong, H.-N. Liu, and P.-H. Tan, "Raman spectroscopy of graphene-based materials and its applications in related devices," Chem. Soc. Rev. **47**, 1822–1873 (2018).

[8]H. Li, J.-B. Wu, F. Ran, M.-L. Lin, X.-L. Liu, Y. Zhao, X. Lu, Q. Xiong, J. Zhang, W. Huang, H. Zhang, and P.-H. Tan, "Interfacial interactions in van der Waals heterostructures of MoS_2 and graphene," ACS Nano **11**, 11714–11723 (2017).

[9]M.-L. Lin, Y. Zhou, J.-B. Wu, X. Cong, X.-L. Liu, J. Zhang, H. Li, W. Yao, and P.-H. Tan, "Cross-dimensional electron-phonon coupling in van der Waals heterostructures," Nat. Commun. **10**, 2419 (2019).

[10]H. Wu, M.-L. Lin, Y.-C. Leng, X. Chen, Y. Zhou, J. Zhang, and P.-H. Tan, "Probing the interfacial coupling in ternary van der Waals heterostructures," npj 2D Mater. Appl. **6**, 87 (2022).

[11]P. H. Tan, W. P. Han, W. J. Zhao, Z. H. Wu, K. Chang, H. Wang, Y. F. Wang, N. Bonini, N. Marzari, N. Pugno, G. Savini, A. Lombardo, and A. C. Ferrari, "The shear mode of multilayer graphene," Nat. Mater. **11**, 294–300 (2012).

[12]X. Zhang, W. P. Han, J. B. Wu, S. Milana, Y. Lu, Q. Q. Li, A. C. Ferrari, and P. H. Tan, "Raman spectroscopy of shear and layer breathing modes in multilayer MoS_2," Phys. Rev. B **87**, 115413 (2013).

[13]J.-B. Wu, Z.-X. Hu, X. Zhang, W.-P. Han, Y. Lu, W. Shi, X.-F. Qiao, M. Ijiäs, S. Milana, W. Ji, A. C. Ferrari, and P.-H. Tan, "Interface coupling in twisted multilayer graphene by resonant Raman spectroscopy of layer breathing modes," ACS Nano **9**, 7440–7449 (2015).

[14]Y. Zhao, X. Luo, J. Zhang, J. Wu, X. Bai, M. Wang, J. Jia, H. Peng, Z. Liu, S. Y. Quek, and Q. Xiong, "Interlayer vibrational modes in few-quintuple-layer Bi_2Te_3 and Bi_2Se_3 two-dimensional crystals: Raman spectroscopy and first-principles studies," Phys. Rev. B **90**, 245428 (2014).

[15]K. Allahverdi, S. Babaev, Ş. Ellialtioğlu, and A. Ismailov, "Raman scattering in layer indium selenide under pressure," Solid State Commun. **87**, 675–678 (1993).

[16]G. Huang, Y. Zhou, Z.-Y. Dong, W.-J. Li, K.-J. Bu, S. Zhou, T. Wang, X.-J. Lü, and X.-J. Chen, "Strongly tunable Raman resonance in InSe under pressure," J. Phys. Chem. C **126**, 6344–6350 (2022).

[17]M. R. Molas, A. V. Tyurnina, V. Zólyomi, A. K. Ott, D. J. Terry, M. J. Hamer, C. Yelgel, A. Babiński, A. G. Nasibulin, A. C. Ferrari, V. I. Fal'ko, and R. Gorbachev, "Raman spectroscopy of GaSe and InSe post-transition metal chalcogenides layers," Faraday Discuss. **227**, 163–170 (2021).

[18]Y.-J. Sun, S.-M. Pang, and J. Zhang, "Layer number-dependent Raman spectra of γ-InSe," J. Phys. Chem. Lett. **13**, 3691–3697 (2022).

[19]C. Song, F. Fan, N. Xuan, S. Huang, C. Wang, G. Zhang, F. Wang, Q. Xing, Y. Lei, Z. Sun, H. Wu, and H. Yan, "Drastic enhancement of the Raman intensity in few-layer InSe by uniaxial strain," Phys. Rev. B **99**, 195414 (2019).

[20]S. Y. Lim, J.-U. Lee, J. H. Kim, L. Liang, X. Kong, T. T. H. Nguyen, Z. Lee, S. Cho, and H. Cheong, "Polytypism in few-layer gallium selenide," Nanoscale **12**, 8563–8573 (2020).

[21]G. Li, X. Wu, Y. Gao, X. Ma, F. Hou, H. Cheng, Q. Huang, Y.-C. Wu, M. C. DeCapua, Y. Zhang, J. Lin, C. Liu, L. Huang, Y. Zhao, J. Yan, and M. Huang, "Observation of ultrastrong coupling between substrate and the magnetic topological insulator $MnBi_2Te_4$," Nano Lett. **22**, 3856–3864 (2022).

[22]G. Froehlicher, E. Lorchat, F. Fernique, C. Joshi, A. Molina-Sánchez, L. Wirtz, and S. Berciaud, "Unified description of the optical phonon modes in N-layer $MoTe_2$," Nano Lett. **15**, 6481–6489 (2015).

[23]X.-F. Qiao, X.-L. Li, X. Zhang, W. Shi, J.-B. Wu, T. Chen, and P.-H. Tan, "Substrate-free layer-number identification of two-dimensional materials: A case of $Mo_{0.5}W_{0.5}S_2$ alloy," Appl. Phys. Lett. **106**, 223102 (2015).

[24]J. Zhang, Z. Peng, A. Soni, Y. Zhao, Y. Xiong, B. Peng, J. Wang, M. S. Dresselhaus, and Q. Xiong, "Raman spectroscopy of few-quintuple layer topological insulator Bi_2Se_3 nanoplatelets," Nano Lett. **11**, 2407–2414 (2011).